

Concurrent Radiotherapy and Tumor Targeting with ^{111}In -HMFG1-F(ab')₂ in Patients with MUC1-positive Non-small Cell Lung Cancer

MICHAEL GARKAVIJ¹, MIROSLAV SAMARZIJA², SVEN B. EWERS¹,
MARKO JAKOPOVIC², STANKO TEZAK² and JAN TENNVALL¹

¹Department of Oncology, University Hospital, SE-22185 Lund, Sweden;

²Clinical Hospital for Lung Diseases and Department of Nuclear Medicine, Zagreb, Croatia

Abstract. *Background:* Combining external radiotherapy (XRT) and radioimmunotargeting might enhance tumor radiation without affecting morbidity, due to different toxicity profiles. *Aim:* To assess ^{111}In -F(ab')₂-HMFG1 biodistribution, the influence of "low-dose" lysine on F(ab')₂ renal uptake and provide data for further concurrent XRT and RIT. *Patients and Methods:* Twenty-three patients received injections of ^{111}In -HMFG1-F(ab')₂, with or without lysine co-infusion, 7 and 21 days after the initiation of XRT. Whole-body images, blood and urine activity were monitored. *Results:* Despite clear visualization of ^{111}In -F(ab')₂-HMFG1, the residence time and absorbed dose in tumors were low. The co-infusion of "low-dose" lysine did not reduce renal uptake, thus contradicting previously published results. The biodistribution differences after the first and the second injection might be attributed to human anti-mouse antibody (HAMA) response or Ag-complexation. *Conclusion:* Low-dose lysine is not feasible. Larger amounts of lysine during extended infusion time are therefore advocated. It is proposed that repeated MAb injection be given during the first fractions of XRT.

Non-small cell lung cancer (NSCLC) remains the leading cause of cancer-related mortality in both men and women worldwide (1). Five-year survival rates for lung cancers remained in the 15% range from 1974 through 1995 (2). However, about 35% of patients with locally advanced disease may potentially be curable (3). Traditional external radiotherapy (XRT) alone has yielded disappointing 5-year

cure rates in this group of patients, mainly due to death from locally advanced disease (4). A substantially larger fraction could be cured if more effective local therapy were available.

Targeted tumor radiation, or radioimmunotherapy (RIT), may produce objective remissions in malignant lymphoma and cure microscopic disseminated solid tumors, but is not effective in manifest solid tumors because these are far less sensitive to radiation and show more heterogeneous growth. Hence, a combined modality approach to therapy has been sought to improve the poor outcome seen with a single modality alone. By combining XRT with radiolabeled antibody treatments the amount of radiation delivered to the tumor can be increased while minimizing associated tissue damage (5, 6). Radiation nephrotoxicity, due to high renal uptake of radiometal-conjugated antibody fragments or peptides, presents a potential problem in tumor radioimmunotherapy (7-9). However, this problem can be successfully overcome, as documented mainly in an experimental situation, by co-injection of amino acids which significantly decrease the uptake of MAb fragments and peptides in the kidneys (10-13). One of very few clinical studies (9) to consider renal uptake of MAb fragments in patients showed that even low doses of amino acids could be as effective (10). Encouraged by these results, the use of "low-dose" lysine co-infusion was taken up in the present study.

The ultimate goal of the study was to provide data for tumor radioimmunotherapy with ^{90}Y -labeled HMFG1-F(ab')₂ in patients with NSCLC receiving external beam radiotherapy. For this reason, the pharmacokinetics and biodistribution of ^{111}In -labeled F(ab')₂ HMFG1-CITC-DTPA were assessed. A secondary aim of the study was to investigate whether co-infusions of lysine-rich amino acids reduce renal uptake of radiolabeled antibody fragments.

Patients and Methods

This was an open label, randomized, parallel, comparative, two-armed study, with or without lysine-rich amino acid infusion. Twenty-six patients were randomized, *i.e.* 13 in each treatment group.

Correspondence to: Michael Garkavij, MD, Ph.D., Department of Oncology, Lund University Hospital, SE-221 85, Lund, Sweden. Tel: +46 46 17 75 20, Fax: +46 46 17 60 75, e-mail: Michael.Garkavij@med.lu.se

Key Words: Lung cancer, ^{111}In HMFG1-F(ab')₂, radiotherapy, biodistribution, lysine.

Twenty-one completed the study: 10 with and 11 without co-infusion. *MAb, radiolabeling and quality control.* MUC1 mucin is a large, transmembrane glycoprotein, the extracellular domain of which is formed by the repeating 20 amino acid sequence, GVTSA PDTRP APG STAPPAH. In normal epithelial cells, the extracellular domain is densely covered with highly branched, complex carbohydrate structures. However, in neoplastic tissue, the extracellular domain is under-glycosylated, resulting in the exposure of a highly immunogenic core peptide epitope PDTRP.

HMFG1 is directed against this epitope, which is expressed by more than 90% of epithelial tumors such as breast, colon, pancreas, prostate, ovary and lung cancer. Among NSCLC, approximately 70% express the PDTRP epitope recognized by HMFG1. The F(ab')₂ of HMFG1 (AS1403) was obtained by enzymatic cleavage of the IgG1 monoclonal antibody HMFG1 using the plant enzyme Ficin (14).

Radiolabeling of the MAb fragment was performed using the labeling kit supplied by Antisoma Research Ltd. (London, UK) and a standard procedure. The HMFG1 F(ab')₂CITC-DTPA, 5 mg, in 0.1 M ammonium acetate was labeled with ¹¹¹In (Mallinckrodt, Petten, Holland) for 10 min at room temperature. The reaction was quenched with an excess of EDTA solution. The radioimmunoconjugate was then purified by size-exclusion gel filtration through a G-25 column. The ¹¹¹In-HMFG1 F(ab')₂CITC-DTPA product was confirmed to consist of more than 98% radioimmunoconjugate monomer using high-performance liquid chromatography (7.8x300 mm molecular sieving column, Phenomenex SEC S3000; Phenomenex, Torrance, CA, USA) eluted in 0.1 M sodium phosphate buffer at pH7 containing 2 mM EDTA at a rate of 0.5 ml/min. The radioimmunoconjugate was detected by ultraviolet absorbance at 250 nm and by radioactivity. The specific activity for ¹¹¹In-HMFG1 F(ab')₂CITC-DTPA was 22-37 MBq/mg. The preparation was stored at +4°C for no longer than 6 h before use.

Patient characteristics and eligibility. Patients had histologically or cytologically verified, measurable NSCLC, TNM stage II-IV, with confirmed MUC1 expression (>10% of tumor cells with positive staining) and were scheduled for XRT (Table I). Other eligibility criteria were a Karnofsky performance score ≥70 %, hematological and biochemical parameters acceptable for the proposed course of XRT, no sensitivity to ¹¹¹In or murine products and no previous exposure to a murine antibody or positive human anti-mouse antibody (HAMA) levels. All standard XRT regimens, viz. 30-60 Gy administered in 2-6 weeks, were accepted. During the pre-study period, the diagnosis and expression of the MUC1 antigen were confirmed by central histopathological /cytological evaluation. On confirmation of eligibility, patients were randomized to treatment with or without lysine-rich amino acid *i.v.* infusion. The mean age of the patients was 61 years with a range of 41 to 80 years. Thirteen of the 23 (57%) had had previous surgery, 16/23 (70%) had had neoadjuvant chemotherapy and 1/23 (4%) had previously undergone XRT. Of the 12 patients (52%) with a histological diagnosis, 4 had large-cell cancer, 3 squamous-cell carcinoma, 3 acinar adenocarcinoma, and 2 other carcinomas of the lung. A cytological diagnosis of NSCLC was confirmed in 11 (48%) of the 23 patients.

Administration of MAb and amino acids in conjunction with XRT. Five mg of HMFG1 F(ab')₂CITC-DTPA, labeled with a 150 MBq imaging dose of ¹¹¹In, was administered over 15-30 sec as a bolus 5 mL *i.v.* injection into a peripheral vein, either with or without an

Table I. *TNM-staging of NSCLC in study patients.*

	Without co-infusion	With co-infusion	Total
TNM Stage IIb	1	2	3
TNM Stage IIIa	4	2	6
TNM Stage IIIb	4	5	9
TNM Stage IV	3	2	5
Total	12	11	23

amino acid co-infusion. All patients received two single injections with a minimum interval of 2 weeks. The two injections were scheduled 7 and 21 days after XRT start. Patients who were randomized to the infusion arm received approximately 3.5 g of lysine and 3.9 g of arginine in 360 ml of 0.9% NaCl solution during a period of 4.5 h. Prior to administration, the amino acid infusion was diluted to an osmolarity of approximately 800 mosm/L to allow for peripheral infusion.

During the study, patients received their scheduled course of XRT, namely, 30 Gy over 2 weeks or 44-60 Gy delivered at a standard daily fractionation of between 1.8 and 2 Gy. Where the XRT course was shorter than 4 weeks, the second study treatment was to be administered after the completion of the XRT, at least 2 weeks after the first dose.

Toxicity was evaluated and recorded using the NCI Common Toxicity Criteria and EORTC scoring guidelines. General adverse events were evaluated using a scale of (1) mild; (2) moderate; (3) severe.

Imaging, dosimetry and biodistribution studies. Radioimmunoscintigrams of whole body, as well as blood and urine samples for local assessment of pharmacokinetics were taken at scheduled time-points during the 96 h following the administration of the labeled antibody. Whole-body images were obtained at approximately 10 min, 1, 4, (+/- 10 min), 24, 48, 72 and 96 h (+/- 4 h).

For each imaging session, the data recorded included the following: acquisition start time, scan speed (cm/min), matrix size, collimator, camera and computer make and model. Blood samples were collected at 10 min, 1 h, 4 h, (+/- 10min) 24 h, 48 h, 72 h and 96 h post injection (+/- 4 h). Daily urine collection was performed for 4 days post injection. Image quantification of Regions of Interest (ROI) using whole-body gamma camera scans included kinetic data and absorbed dose estimates for tumor(s), normal target organs and residence times for the urinary bladder, red marrow and whole body. The resulting time activity data, together with blood and urine data, were modeled to possess residence times. Dose estimates were produced using the Cristy-Eckerman radiation transport phantoms and standard MIRD methodology (15, 16). Dose estimates were mass-scaled based on the body mass of the individual patient. Concerning "Image quantification methods" and "Biokinetic modeling" used, see Appendix 1.

Safety. The main safety variables were the National Cancer Institute (NCI) Common Toxicity Criteria v.2, laboratory abnormalities and spontaneously reported adverse events. EORTC acute radiation toxicity scoring was used to record radiation-related events.

Table II. Expression of MUC1 antigen in tumors.

Percent of stained cells	Intensity of staining					
	Immunohistochemistry			Immunocytochemistry		
	+	++	+++	+	++	+++
11-30%	1 (MC)	-	-	2	2	-
31-60%	2 (SC, LC)	2 (AC, SC)	-	-	-	-
>60 %	3 (2xLC, MC)	2 (AC, LC)	2 (AC, SC)	4	3	-

SC, squamous-cell ca; LC, large-cell ca; AC, adenocarcinoma; MC, miscellaneous type.

Statistical methods. There was no formal sample size calculation for this study. It was expected that 10 evaluable patients per group would be a sufficient sample size to support the dosimetry analysis and bio-kinetic modeling, and to allow identification of any inter-patient differences.

All calculations were done using SAS Version 8.2 or Microsoft EXCEL.

The mean, median, standard deviation, minimum and maximum for the total population were given. For continuous variables, differences were assessed using a two-sample *t*-test where distributional assumptions held, and using a Mann-Whitney test otherwise. For categorical variables, differences between the amino acid-rich intravenous co-infusion groups were assessed using Fisher's exact test. The mean levels for the total population were calculated and a 95% confidence interval presented. For each statistical test, an observed significance level was quoted. Where this value was less than 0.05, 0.01 or 0.001, attention was drawn to the fact using the conventional "*", "**" or "***" annotation.

Results

Tumor biopsies from 12 patients and tumor cytology from 11 patients were evaluated for MUC1 expression. The intensity of the staining is presented in Table II.

Safety. In general, the toxicities and adverse events seen and the types of concomitant medications taken were in line with expectations for lung cancer patients receiving XRT after chemotherapy. Twelve (57%) of the 21 patients receiving 2 injections of the study drug had liver toxicities of grade 1. There were 3 (14%) grade 1 renal toxicities and 1 (5%) cardiac toxicity of grade 1. No serious adverse events were considered to be related to the study drug. One patient was withdrawn from the study due to an adverse event (high human anti-mouse antibody (HAMA) levels after injection 1). There were no deaths during the period of the study treatment.

Biodistribution results. The percentage of the injected dose as a function of time was determined for the whole body,

blood, tumors, radiosensitive organs such as kidneys, liver, lungs and bone marrow (assessed from cervical spine, lumbar spine, humeral and femoral heads).

The whole-body curve was monophasic ($t_{1/2} > 96$ h) and showed slow activity excretion. There were no significant differences in whole-body content between the first and second injections or between patients receiving or not receiving amino acid infusion.

Blood kinetics. Blood clearance displayed a bi-exponential activity curve after both injections, independent of whether the patients received the co-infusion (Figure 1). The activity of $^{111}\text{In-HMFG1 F(ab')_2}$ was cleared from the blood after injection 1 with a distribution half-life ($t_{1/2 \alpha}$) of 9.1 h and a terminal half-life ($t_{1/2 \beta}$) of 51.5 h. After the second injection, blood clearance showed a distribution half-life ($t_{1/2 \alpha}$) of 8.7 h and a terminal half-life ($t_{1/2 \beta}$) of 50.4 h. Rapid clearance of activity from the blood ($t_{1/2 \alpha} = 1.3$ h; $t_{1/2 \beta} = 27.3$ h) followed by greatly increased retention of the activity in the liver was observed in 5 patients (Figure 1, triangles) after injection 2. Only 1 of these patients had a slightly increasing HAMA concentration (82 ng/ml after injection 1 and 164 ng/ml after injection 2), with normalization after 6 weeks.

Urinary excretion. Total urinary excretion of radioactivity, determined by the assay of urine samples over 96 h, ranged from about 6% to approximately 50% of the injected activity (average about 19%). The difference in total urinary excretion between injection 1 and injection 2 was less than 3% of the injected activity. It was significantly increased in 5 patients with more pronounced clearance (Table III), but was nevertheless delayed in comparison to the fall of the activity in the blood (possibly due to MAAb complexation and accumulation in the liver). A concomitant lysine-rich amino acid infusion had little effect on urinary excretion.

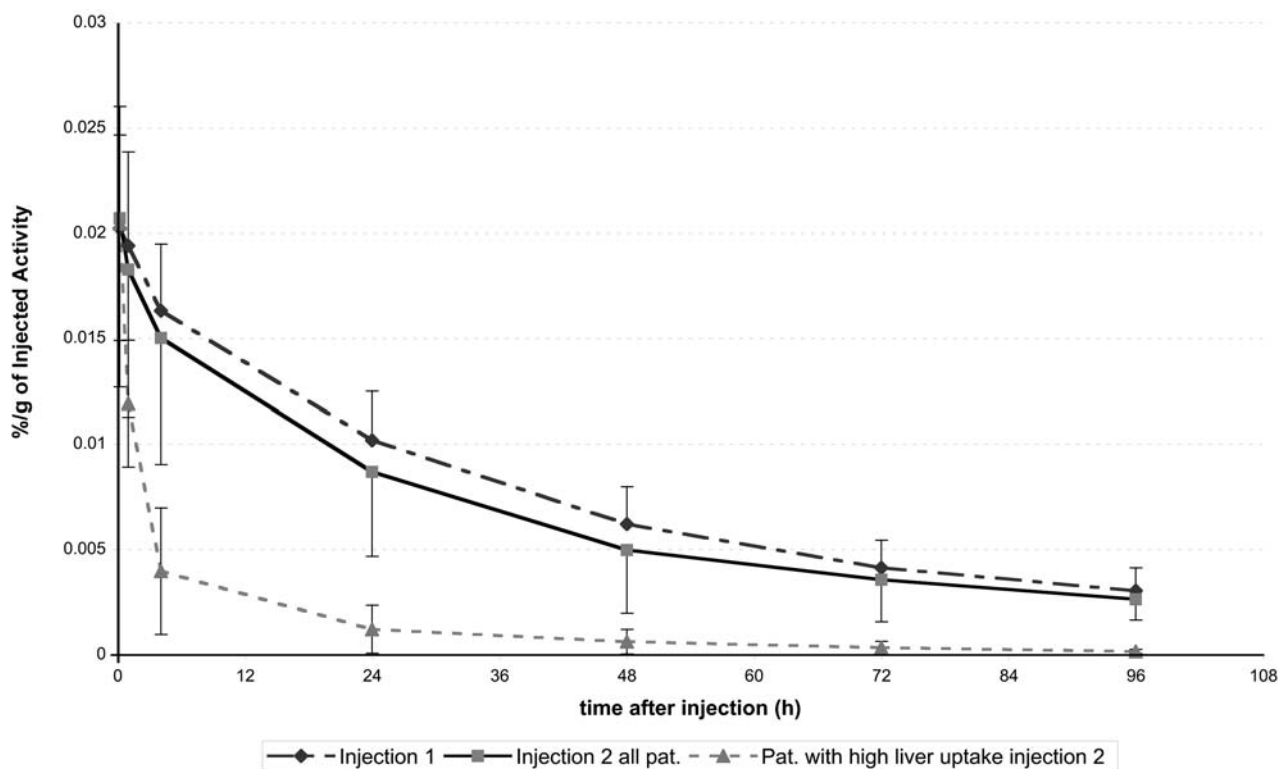


Figure 1. Blood activity clearance (%g of injected activity) after injection 1 and 2. Rapid blood clearance ($t_{1/2\alpha}=1.3$ h; $t_{1/2\beta}=27.3$ h) followed by greatly increased activity retention in the liver was observed in 5 patients (triangles) after injection 2.

Table III. Average urinary excretion (%LA).

Time after injection (h)	24	48	72	96
Injection 1	3.2%	9.0%	15.3%	21.0%
Injection 2	4.3%	11.0%	18.4%	24.8%
Data concerning 5 patients with rapid blood clearance after injection 2 showed as triangles in Figure 2	8.3%	18.5%	27.9%	34.9%

Tumor uptake. Clear tumor uptake was seen in 14 (63.6%) of the 22 patients after the first injection and in 10 (47.6%) of 21 patients after the second injection. It is possible that additional patients had tumor uptake which was obscured by vascular structures immediately adjacent to the heart. Maximum uptake was seen at 48 h after injection 1. Activity uptake after injection 2 was low, decreasing gradually over 96 h (Figure 2).

Liver uptake. For both injections, the organ with the largest uptake was the liver. The uptake was significantly higher at

all post-injection time-points after the second as compared to the first injection (Table IV).

For the first injection, the liver showed the largest uptake with an average peak uptake of 15%. For the second injection, the organ that showed the largest uptake was also the liver (average peak uptake 29%).

There was a much wider discrepancy in peak liver uptakes after injection 2. Six patients demonstrated what might have been an MAb and circulating Ag immune-complex, or HAMA-like response, with correspondingly large liver uptakes after the second injection. The mean levels of HAMA for these patients were 0 ng/ml at screening and 22 ng/ml (median 10) at the follow-up after injection 1. HAMA increased slightly (median 19, $p=0.14$) after injection 2.

Peak liver uptake following the second injection was greater than 70% in 1 patient and greater than 50% in several others. Concomitant lysine-rich amino acid infusion had no effect on liver uptake.

Uptake in the kidneys. There were statistically significant differences between the two study arms for AUC (0-96 h) and at 24, 48 and 72 h post-injection (p.i.). In each case, patients who received lysine-rich amino acid infusion had

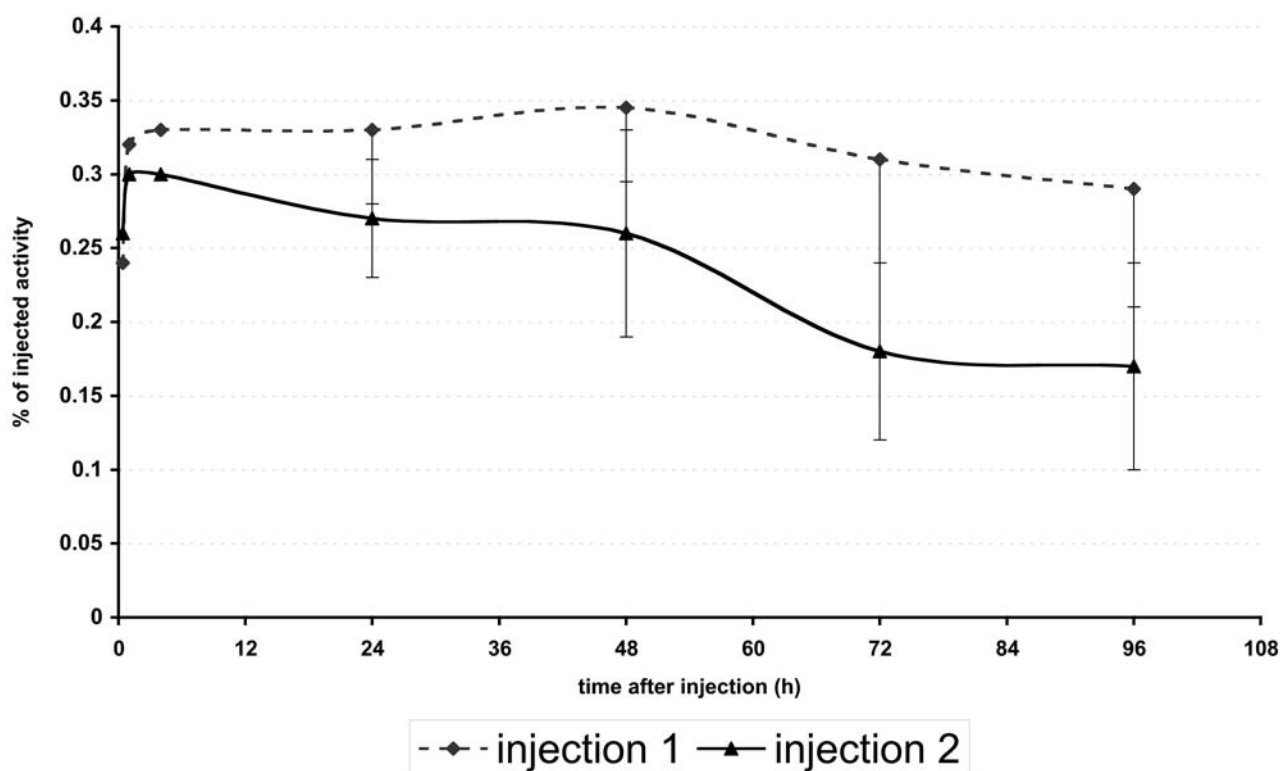


Figure 2. Average tumor uptake (percentage of injected activity) as a function of time for each injection. Maximum uptake found at 48 h after injection 1. The uptake after injection 2 was low, decreasing gradually over 96 h.

higher renal uptakes (Table V). For the same 4 analyses (AUC 0-96 h and at 24, 48 and 72 h p.i.) there was a significant difference between injections, with higher uptakes following the first injection. There were no statistically significant differences apparent at 10 min, 1, 4 and 96 h p.i.

Activity residence times. Statistically significant, higher activity residence times were observed after the first compared with the second injection for the lungs, red marrow and remaining tissues. The liver had significantly higher residence times after injection 2 ($p < 0.001$). The average residence time in the tumor was lower than in lung tissue ($p < 0.05$).

Dosimetry estimates. The average absorbed doses from the $^{111}\text{In-}^{90}\text{Y-HMFG1 F(ab')_2\text{CITC-DTPA}}$ in tumors were low (3.1 and 2.4 mGy/MBq after injection 1 and 2, respectively). The largest, average absorbed doses after the first injection were 5.5 mGy/MBq for the kidneys, 3.6 mGy/MBq for the liver and 3.0 mGy/MBq for the spleen. For the second injection, the largest absorbed doses were for the liver, kidneys and spleen (6.8 mGy/MBq, 4.5 mGy/MBq and 2.7 mGy/MBq, respectively). Absorbed doses estimated for injection 1 were generally similar to those for injection 2 with

Table IV. Comparison of liver uptake after injection 1 and injection 2 as a percentage of injected activity.

	Injection 1 (mean)	Injection 2 (mean)	Mean difference	<i>p</i>
AUC (0-96 h)	14.48	27.73	-13.25	0.0013 **
10 min	11.09	17.91	-6.82	0.013 *
1 h	13.98	22.25	-8.28	0.03 *
4 h	12.97	26.01	-13.04	0.013 *
24 h	14.88	29.46	-14.58	0.002 **
48 h	15.87	29.68	-13.80	0.002 **
72 h	14.81	27.44	-12.63	<0.001 ***
96 h	13.28	25.69	-12.41	<0.001 ***

*Significant at the 5% level

**Significant at the 1% level

***Significant at the 0.1% level

the exception of the liver. Absorbed doses in the kidneys were about 26% higher with the infusion in the first injection, and about 44% larger with the infusion after the second injection. Absorbed doses in the liver were about 3% lower with the infusion after the first injection, and about 27% larger with the infusion after the second injection.

Table V. Summary of kidney uptake for both injections as a % of injected dose.

Time after injection	Mean ^a		Difference between means ^b				<i>p</i> ^c
	Without co-infusion	With co-infusion	Mean	sd	95%	CI	
AUC (0-96 h)	3.02	3.76	0.73	0.26	0.19	1.27	0.011 **
10 min	1.55	1.59	0.04	0.10	-0.17	0.24	0.70
1 h	1.78	1.65	0.13	0.10	-0.07	0.34	0.18
4 h	2.00	2.33	0.33	0.16	-0.01	0.67	0.67
24 h	3.12	3.81	0.69	0.28	0.11	1.27	0.02 *
48 h	3.30	4.40	1.10	0.30	0.48	1.72	0.002 **
72 h	3.29	4.08	0.79	0.35	0.07	1.51	0.03 *
96 h	2.96	3.40	0.45	0.29	-0.17	1.06	0.15

^aEstimated from ANOVA model with factors for patient and injection

^bWith co-infusion minus without co-infusion

^c*p*-value for injection taken from ANOVA model

*Significant at the 5% level

**Significant at the 1% level

HAMA. Human anti-mouse antibody was detectable in 6 out of 12 patients (50%) in the group without co-infusion and 3 (25%) had levels greater than 50 ng/ml. One patient in the co-infusion group had detectable HAMA (12 ng/ml) at screening but was excluded from the study for other reasons. Seven of the remaining 10 patients (70%) in the co-infusion group demonstrated HAMA and 4 (40%) had levels greater than 50 ng/ml. One patient had detectable HAMA (62 ng/ml) at screening. The patient with the highest HAMA value (17837 ng/ml), occurring at the end of the first week following the first injection, was withdrawn after the first dose for safety reasons.

Discussion

Clinical studies on radioimmunotargeting (RIT) of solid tumors have, in general, revealed limited efficacy. Combined modalities such as concomitant XRT and radiolabeled antibody fragments might provide an enhanced effect on tumor irradiation, as the toxicity profiles of these two modalities do not overlap.

The renal uptake of radiolabeled MAb fragments and peptides presents a problem in tumor RIT, particularly with intracellularly-retained isotopes (7, 8). Successful reduction of the renal uptake of MAb fragments by amino acid infusion in adult baboons and patients have been reported (10, 11). The infusion of large amounts (about 50 g) of amino acids reduced renal exposure during peptide-based radiotherapy and allowed higher absorbed doses to tumors (13). The prolongation of the infusion from 4 to 10 h further enhanced the protective effect on the kidneys (13). Behr *et al.* have demonstrated that the renal uptake was significantly

reduced after co-infusion of only 4.5 g lysine-glutamate together with 5.0 g arginine (9). The reduction of kidney uptake was achieved even at considerably lower doses that were safe and effective in animals (10, 12). The mechanism seems to rely on an inhibition of the re-absorption of tubularly-filtered proteins by the proximal tubule cells. These conclusions encouraged us to further investigate the low-dose amino acid co-infusion to reduce renal uptake. The results above were not reproduced in our study, *i.e.* when patients received co-infusion of approximately the same low doses of lysine and arginine. Considering the half-life of the MAb fragment and that of the lysine-rich infusion, a low-dose co-infusion is unlikely to be of benefit, and a more extended infusion time should be evaluated.

Experimental RIT with ¹¹¹In-AUA1 MAb against colon adenocarcinoma showed a potential value of XRT to increase MAb uptake by the increased vascular permeability of the tumor vasculature soon after the irradiation exposure (6). A clinical study of MAb-guided targeting of NSCLC using the same ¹¹¹In-labeled HMFG1 F(ab')₂ fragment, but without concomitant XRT, proved clear tumor visualization with residence times in the tumor longer than those in most normal tissues (17). The present study also showed good tumor visualization in the majority of the patients (63.6% after the first injection), but the residence time of the radioactivity in the tumor was short. Several studies (5, 18, 19) have emphasized the importance of optimal sequencing when combining XRT and RIT. The activity uptake in human colon carcinoma xenografts was increased by almost 50% when the MAb was present in the blood at the start of external beam irradiation (20). Five days into a fractionated irradiation protocol, MAb uptake

was reduced, falling more significantly on day 10 (20). Concurrent administration of RIT and XRT produced greater tumor shrinkage than delayed or sequential injections of radiolabeled MAb (21). Furthermore, the close association of RIT and XRT without delay was more efficient than a therapy with a treatment-free interval of 2 weeks (5). A feasible explanation is that external beam irradiation may hamper the diffusion of therapeutic agents such as MAb or F(ab) by reducing interstitial fluid transport in tumors (19). In our study, the patients at the time of the first injection received about 10 Gy of XRT to the tumor and 30 Gy at the time of the second injection of F(ab')₂, which may well impair tumor targeting.

The study also showed activity accumulation in organs of the reticular-endothelial system. There were several patients with a liver uptake greater than 50% of the injected activity, with a peak at 48 h p.i. However, the repeated use of the F(ab')₂ might be immunogenic. HAMA may neutralize the injected MAb directly by immune complex formation, which could lead to rapid clearance or to hypersensitivity reactions (22-24). We revealed a rapid and statistically significant increase in liver uptake after the second injection, as would be expected if immune complexes were being formed between the F(ab')₂ fragment and anti-murine IgG or MUC1 Ag from degraded tumor after XRT. One patient demonstrated a marked possible immunological response (HAMA value of 17837 ng/ml) at the end of the first week following the first injection of F(ab')₂, resulting in withdrawal from the study. HAMA was detected at values above 50 ng/ml in an additional 5 patients, 3 of whom had higher HAMA values after the second dose than after the first. This level of immunogenicity has not been reported by other investigators using the same F(ab')₂ antibody (17). One remotely possible explanation might be the use of ficin, a plant enzyme, to produce the HMFG F(ab')₂. On the other hand, HAMA levels less than 100 ng/ml are not considered to affect the outcome of the therapeutic or diagnostic procedures (25, 26). Since HAMA did not increase after the first injection in 5 patients with rapid excretion and high liver accumulation, the biological relevance of low HAMA values (50-100 ng/ml) on biodistribution parameters is less likely.

Conclusion

The low-dose amino acid co-infusion did not result in the reduction of renal uptake, in contradiction to the results supporting "low-dose" co-infusion (9). Differences in the biodistribution after the first and second injection might be attributed to HAMA-response or Ag-complexation. Despite obvious tumor imaging with $^{111}\text{In-HMFG1 F(ab')}_2$, the residence time and absorbed dose in tumors were low. This may reflect unfavorable timing between the injection of the radiolabeled F(ab')₂ and initiation of the radiotherapy. A

closer conjugation, with no time delay, of RIT and XRT, as well as an increased amount of amino acids and an extended infusion time, should be considered in future protocols.

Acknowledgements

Supported by Antisoma Research Ltd., West Africa House, London W5 3QR, UK, and in part by grants from the Swedish Cancer Society; the Mrs. Berta Kamprad Foundation; the Gunnar, Arvid and Elisabeth Nilsson Foundation; Foundations of the Lund Health District Organization and Lund University Medical Faculty, Sweden.

The authors express gratitude to Ms. K.Connor, Dr. S.Hadfield and Dr. N.S.Courtenay-Luck, Antisoma Research Ltd., West Africa House, London W5 3QR, UK for their helpful discussions and valuable consultations in the preparation of the manuscript. Furthermore, the authors thank Richard Sparks, Ph.D., CDE Dosimetry Services, Inc.10000 Cheltenham Drive, Knoxville, TN 37922, USA for the dosimetric evaluation of the study results.

APPENDIX 1.

Image quantification methods. Regions of interest (ROI), appropriate background, and obstructed ROIs were drawn for all organs, tissues and tumors showing uptake above "background" tissues. The image quantification was performed according to the methodology presented in MIRD Pamphlet No. 16 (15) except that the calibration factor to transform counts to activity was determined using the adjusted geometric mean of the total body counts in the first image. In the MIRD 16 methodology, ROI counts are adjusted by attenuation correction derived from the transmission and reference transmission images. Region counts are also adjusted for activity containing underlying and overlying tissue that is not part of the organ being quantified, and for self-attenuation. Total body region counts are also corrected for off body background counts. Appropriate normalizations of region sizes for organ and adjacent regions were made.

The general form of the equations used were as follows:

$$A_{Organ} = F \left(\left[\sqrt{\frac{I_{ROI_A} I_{ROI_P}}{T_{ROI}}} \right] \right) \frac{f_{Organ}}{C}$$

$$F = \left\{ \left[1 - \left(\frac{I_{ADJ_A}}{I_{ROI_A}} \right) \left(1 - \frac{t_j}{t} \right) \right] \left[1 - \left(\frac{I_{ADJ_P}}{I_{ROI_P}} \right) \left(1 - \frac{t_j}{t} \right) \right] \right\}$$

$$T_{ROI} = \frac{I_T}{I_{RT}}$$

$$f_{Organ} = \frac{\frac{\mu_j t_j}{2}}{\sinh\left(\frac{\mu_j t_j}{2}\right)}$$

Where:

A_{ROI} =Activity in the ROI, I_{ROIA} =Anterior ROI counts, I_{ADJA} =Anterior adjacent ROI count, I_{ROIp} =Posterior ROI counts, I_{ADJP} =Posterior adjacent ROI counts, I_T =Transmission ROI counts through patient, I_{RT} =Reference transmission ROI counts, t =Patient thickness, t_j =Organ being quantified thickness, T_j =attenuation coefficient for organ being quantified, C =Calibration factor, based on 1st image whole-body counts (counts/unit activity), f_{Organ} =Source attenuation factor.

For all above terms involving whole body, the definitions are identical, with the region of interest being whole body. The available transmission scans were performed with a ^{57}Co flood source. The transmission factors were determined by making the appropriate corrections based on a flood source phantom study using both ^{57}Co and ^{111}In flood sources. For patients where no transmission scan was performed, the above methodology was modified by the removal of the transmission (T), and source self-attenuation (f-Organ) factors. Additionally, for patients where no transmission scan was performed, theoretical attenuation correction and self-attenuation was determined for lungs only.

Biokinetic modeling. Kinetic data for heart contents, kidneys, liver, lungs, cervical spine, lumbar spine, humeral heads, femoral heads, spleen, testes, bladder, small intestine contents, upper large intestine contents, lower large intestine contents, remaining tissues, tumors and whole body for HMFG1 F(ab')₂CITC-DTPA for 22 patients (2 injections for all but 1 patient who received a single injection, for a total of 43 complete data sets) were determined using the image quantification methodology described above. These data, along with blood time activity data, were fit in a least squares sense with sums of exponentials of the form:

$$A(t) = \sum_i f_i e^{-\lambda_i t}$$

Urinary excretion data were fit using the sums of exponentials of the form:

$$A(t) = \sum_i f_i - \sum_i f_i e^{-\lambda_i t}$$

Once these data had been fit, residence times were determined by integration of these empirically determined functions from time equal zero to infinity. The residence time for the urinary bladder was found by integration of the empirically determined function, with the addition that the activity value was "forced" to zero at constant intervals of

4.8 h (16). The remainder of body residence times were determined by subtraction of appropriate organ residence times from whole body residence times. The red marrow residence time was determined based on appropriate selection of ROIs drawn on the upper thirds of the humeri and femurs, and the entire lumbar and cervical spine regions, which were assumed to contain 2.3%, 6.7%, 12.3% and 3.9%, respectively (ICRP-70) of the total red marrow.

References

- 1 American Cancer Society: Cancer Facts & Figures 2003. <http://www.cancer.org/downloads/STT/CAFF2003PWSecured.pdf>.
- 2 Ferlay J, Parkin DM, Pisani P and Globocan L: Cancer Incidence and Mortality World-wide, IARC Press: Lyon 1998 and Landis SH *et al*: CA Cancer J Clin 49: 8-31, 1999.
- 3 Greenlee RT, Murray T, Bolden S and Wingo PA: The Surveillance Research Program of the American Cancer Society's Department of Epidemiology and Surveillance Research reports its annual compilation of estimated cancer incidence, mortality, and survival data for the United States in the year 2000. CA Cancer J Clin 50: 7-33, 2000.
- 4 Stevens CW, Lee JS, Cox J and Komaki R: Novel approaches to locally advanced unresectable non-small cell lung cancer. Radiother Oncol 55: 11-18, 2000.
- 5 Buchegger F, Roth A, Allal A *et al*: Radioimmunotherapy of colorectal cancer liver metastases: combination with radiotherapy. Ann NY Acad Sci 910: 263-270, 2000.
- 6 Kalofonos H, Rowlinson G and Epenetos AA: Enhancement of monoclonal antibody uptake in human colon tumor xenografts following irradiation. Cancer Res 50: 159-163, 1990.
- 7 Behr TM, Goldenberg DM and Becker W: Reducing the renal uptake of radiolabeled antibody fragments and peptides for diagnosis and therapy: present status, future prospects and limitations. Eur J Nucl Med 25: 201-212, 1998.
- 8 DeNardo SJ, O'Donnell RT and DeNardo GL: Potential use of amino acid cocktails to reduce renal tubular reabsorption of radioconjugates. J Nucl Med 37: 829-833, 1996.
- 9 Behr Th, Becker W, Sharkley R *et al*: Reduction of renal uptake of monoclonal antibody fragments by amino acid infusion. J Nucl Med 37: 829-833, 1996.
- 10 Behr Th, Sharkey RM, Sgouros G *et al*: Overcoming the nephrotoxicity of radiometal-labeled immunoconjugates: improved cancer therapy administered to a nude mouse model in relation to the internal radiation dosimetry. Cancer 80: 2591-2610, 1997.
- 11 Carrasquillo J, Lang L, Whatley M *et al*: Aminosyn II effectively blocks renal uptake of ^{18}F -labelled anti-tac disulfide-stabilised Fv. Cancer Res 58: 2612-2617, 1998.
- 12 Kabayashi H, You TM, Kim IS *et al*: Favorable effect of lysine on biodistribution and metabolism of Tc-99m dsFv. J Nucl Med 37: 129s, 1996.
- 13 Jamar F, Barone R, Mathieu I *et al*: ^{86}Y -DOTA(0)-D-Phe1-Tyr3-octreotide (SMT487) - a phase 1 clinical study: pharmacokinetics, biodistribution and renal protective effect of different regimens of amino acid co-infusion. Eur J Nucl Med 30: 510-518, 2003.
- 14 Zotter S, Hageman PC, Lossnitzer A, Mooi WJ and Hilgers J: Tissue and tumor distribution of human polymorphic epithelial mucin. Cancer Res 11: 55-101, 1988.

- 15 Siegel JA, Thomas SR, Stubbs JB *et al*: MIRD pamphlet no. 16: Techniques for quantitative radiopharmaceutical biodistribution data acquisition and analysis for use in human radiation dose estimates. *J Nucl Med* 40: 37-61S, 1999.
- 16 Cloutier RJ, Smith SA, Watson EE, Snyder WS and Warner GG: Dose to the fetus from radionuclides in the bladder. *Health Phys* 25: 147-161, 1973.
- 17 Kalofonos HP, Sivolapenko GB, Courtenay-Luck NS *et al*: Antibody guided targeting of non-small cell lung cancer using ^{111}In -labeled HMFG1 F(ab')₂ fragments. *Cancer Res* 48: 1977-1984, 1988.
- 18 Buchegger F, Rojas A, Delaloye AB, Vogel CA *et al*: Combined radioimmunotherapy and radiotherapy of human colon carcinoma grafted in nude mice. *Cancer Res* 55: 83-89, 2000.
- 19 Znati CA, Rosenstein M, McKee TD *et al*: Irradiation reduces interstitial fluid transport and increases the collagen content in tumors. *Clin Cancer Res* 9: 5508-5513, 2003.
- 20 Ruan S, O'Donoghue J, Larson SM *et al*: Optimizing the sequence of combination therapy with radiolabeled antibodies and fractionated external beam. *JNM* 41: 1905-1912, 2000.
- 21 Sun LQ, Vogel CA, Mirimanoff RO, Coucke P, Mach JP and Buchegger F: Timing effects of combined radioimmunotherapy and radiotherapy on a human solid tumor in nude mice. *Cancer Res* 57: 1312-1319, 1997.
- 22 Mojiminiyi SA, Shepstone BJ and Soper ND: Human antimurine antibodies (HAMA) *in vivo* complex formation and the outcome of immunoscintigraphy. *J Nucl Med* 31: 381-382, 1990.
- 23 Rettenbacher L and Galvan G: Anaphylactic shock after repeated injection of $^{99\text{m}}\text{Tc}$ -labeled CEA antibody (in German). *Nuklearmedizin* 33: 127-128, 1994.
- 24 Sakahara H, Reynolds JC, Carrasquillo JA *et al*: *In vitro* complex formation and biodistribution of mouse antitumor monoclonal antibody in cancer patients. *J Nucl Med* 30: 1311-1317, 1989.
- 25 Frodin J-E, Faxas M-E, Hagström B *et al*: Induction of anti-idiotypic (ab2) and anti-anti-idiotypic (ab3) antibodies in patients treated with the mouse monoclonal antibody 17-1A (ab1). Relation to the clinical outcome – an important antitumoral effector function? *Hybridoma* 10: 421-431, 1991.
- 26 Gruber R, van Haarlem LJ, Warnaar SO, Holz E and Riethmuller G: The human antimouse immunoglobulin response and the anti-idiotypic network have no influence on clinical outcome in patients with minimal residual colorectal cancer treated with monoclonal antibody CO17-1A. *Cancer Res* 60: 1921-1926, 2000.

Received June 2, 2005

Accepted September 1, 2005